Urol Res (2009) 37:323–329
DOI 10.1007/s00240-009-0213-5

ORIGINAL PAPER

Proteomic analysis of a matrix stone: a case report

Benjamin K. Canales · Lorraine Anderson · LeeAnn Higgins · Chris Frethem · Alice Ressler · Il Won Kim · Manoj Monga

Received: 30 December 2008 / Accepted: 14 August 2009 / Published online: 4 September 2009

Abstract Matrix stones are radiolucent bodies that present as soft muco-proteinaceous material within the renal collecting system. Following wide-angle X-ray diffraction (XRD) and scanning electron microscopy (SEM), we homogenized a surgically removed matrix stone, extracted and purified protein, and analyzed samples using tandem mass spectrometry for proteomic composition. Resulting spectra were searched using ProteinPilot 2.0, and identified proteins were reported with >95% confidence. Primary XRD mineral analysis was a biological apatite, and SEM revealed fibrous, net-like laminations containing bacterial, cellular, and crystalline material. Of the 33 unique proteins identified, 90% have not been previously reported within matrix stones and over 70% may be considered inflammatory or defensive in nature. Characterization of other matrix stone proteomes, in particular from non-infectious populations, may yield insights into the pathogenesis of this rare stone as well as the mineralogical process that occurs within crystalline calculi.

Keywords Proteome · Nephrolithiasis · Inflammation · Matrix stone

B. K. Canales · M. Monga
Department of Urologic Surgery,
University of Minnesota, Minneapolis, MN, USA

L. Anderson · L. Higgins
Department of Biochemistry,
Molecular Biology and Biophysics,
University of Minnesota, Minneapolis, MN, USA

C. Frethem · A. Ressler
Characterization Facility, College of Physical Sciences,
Engineering and Mathematics, University of Minnesota,
Minneapolis, MN, USA

I. W. Kim
Department of Chemical and Environmental Engineering,
Soongsil University, Seoul, Korea

B. K. Canales
Center for the Study of Lithiasis and Pathological Calcification,
University of Florida, Gainesville, FL, USA

B. K. Canales (✉)
Department of Urology, University of Florida,
1600 SW Archer Rd, N-213, PO Box 100247,
Gainesville, FL 32610-0247, USA
e-mail: Benjamin.canales@urology.ufl.edu

Introduction

In the early 1950's, Boyce and Sulkin [1] were the first to extract organic substances from calcium salts that had precipitated within the human urinary tract. They postulated that, although found in quantities of <3% of total stone weight, this organic "matrix" directed the biomineralization process in an orderly manner. Matrix stones, originally described in 1908 [2], are rare calculi that present not as crystalline solids but as soft, proteinaceous material within the kidney collecting system. Almost the converse of stone matrix, matrix stones have little mineral and are primarily composed of organic material that could be ideal for protein extraction. They have been identified in patients with recurrent urinary tract infections and in proteinuric patients with glomerulonephritis and end-stage kidney disease on hemodialysis [3]. In an attempt to understand the factors responsible for matrix stone formation, our group determined the mineral, topographical, and proteomic composition of a surgically extracted matrix stone using modern identification technology.

Materials and methods

Stone collection

A 44-year-old diabetic female presented to our stone clinic with recurrent *Proteus mirabilis* urinary tract infections and left flank pain. Abdominal imaging demonstrated a 1.2 cm renal stone with a hypodense center located in the left renal pelvis (Fig. 1). The patient was enrolled in an IRB-approved, prospective stone bank study, and ureteroscopic extraction revealed a mucus-like, gritty stone consistent with matrix stone (Fig. 1). The specimen was washed in saline and immediately frozen at −80°C in a standard protease inhibitor (Sigma-Aldrich, Oakville, ON, Canada).

X-ray diffraction

Epoxy-embedded matrix stone mineral composition was confirmed by wide-angle X-ray diffraction using a Bruker-AXS General Area Detector Diffraction System (GADDS, Karlsruhe, Germany) with Cu radiation generated at 45 kV and 40 mA. Two frames of diffraction data (10–40° and 40–70°) were collected with a Hi-Star multi-wire 2-D area detector each for 10,000 s. Each frame was collected by placing the detector at the center of the 2θ range using precise-beam positioning with a video-microscope and laser pointer. Data were integrated to display a typical 2θ plot versus intensity. Spectral data were analyzed using JADE® 7.0 software (Material Data Incorporated, Livermore, CA) and reconstructed using Mercury® Version 1.4.2 software (Cambridge Crystallographic Data Centre, United Kingdom). A representative example of stone matrix mineral content (Fig. 2) was compared to known pure crystal samples of biological apatite [4] and synthetic apatite, prepared according to a known protocol [5]. All diffraction patterns were plotted using Origin® Version 6.0 (OriginLab, Northampton, MA).

Scanning electron microscopy

Five separate 4 × 4 mm samples were placed in a 2.5% glutaraldehyde/0.1 M sodium cacodylate buffer and secondarily fixed in 1% osmium tetroxide. Samples were then dehydrated by graded ethanol series (50, 70, 80%, 95 × 2, 100% × 2) on a slow rotator. One sample was dried in liquid CO_2 using the critical-point method and freeze-cracked in the 95% ethanol step to reveal its inner aspects. One sample was thin sectioned (6 nm) and sputter coated with 60–40% gold–palladium for secondary electron imaging. Three remaining specimens were embedded in an epoxy resin, Poly/Bed® 812 (Polysciences, Inc.m Warrington, PA) for mineral analysis.

Chemicals

Reagent grade chemicals were purchased from Sigma-Aldrich (Oakville, ON, Canada) or Fisher Scientific (Nepean, ON, Canada). Protein denaturant (0.2% sodium dodecyl sulphate [SDS]), reducing reagent (50 mM Tris-2-carboxyethyl-phosphine [TCEP]), cysteine blocking reagent (200 mM methyl methane-thiosulfonate [MMTS]), dissolution buffer (0.5 M triethylammonium bicarbonate [TEAB], pH 8.5) for trypsin digestion, and trypsin were obtained from Applied Biosystems (Foster City, CA). For LC-MS, acetonitrile (ACN) was purchased from Burdick and Jackson (Muskegon, MI), and formic acid was acquired from Acros (Geel, Belgium).

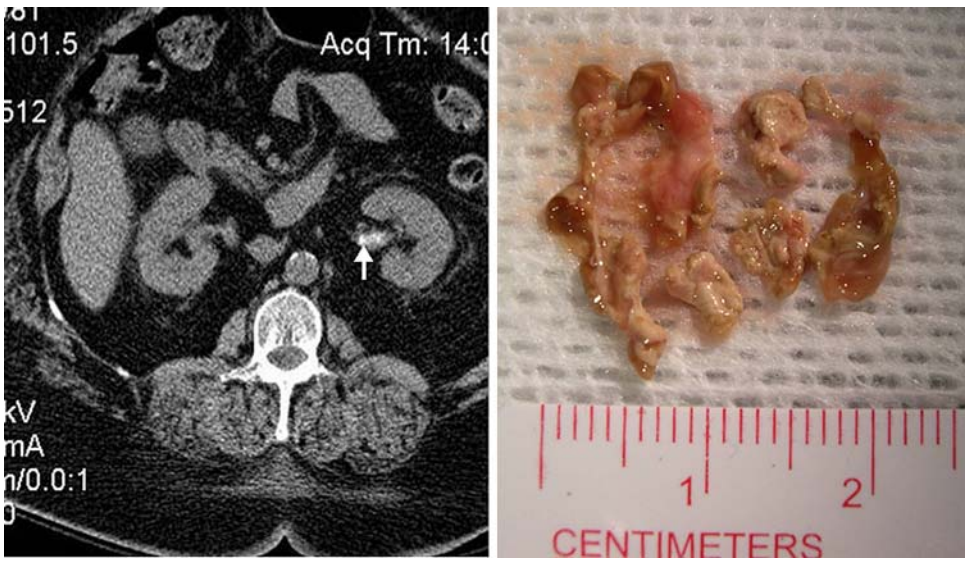

Fig. 1 Non-contrast, abdominal computed tomography of left renal pelvis matrix stone (*arrow, left inset*). Photograph of matrix stone extracted ureteroscopically from a diabetic female (*right inset*), ruler in centimeter

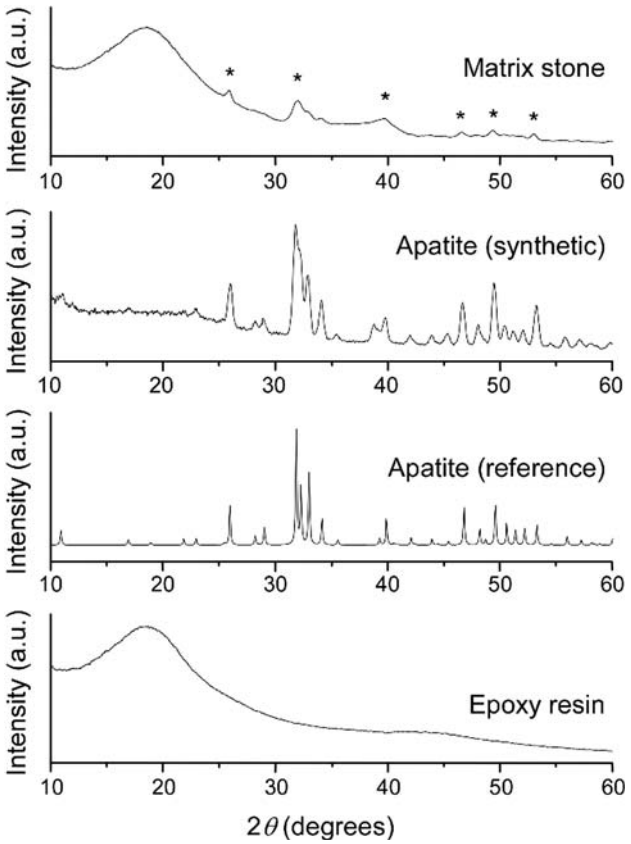

Fig. 2 Stacked plot of four X-ray diffraction patterns. (*Top*) Matrix stone peaks (*) correspond to biological apatite mineral with intense peak at 19° corresponding to embedded epoxy resin (*bottom*)

Protein extraction

Using a tissue morcellator, matrix stone was homogenized and 2 ml of solution was mixed with 400 µl SDS reducing buffer (2% SDS, 0.06 M Tris HCl, 10% glycerol, 5% beta-mercaptoethanol) and heated to 100°C in a water bath (30 min). Samples were centrifuged (700×*g*, 15 min, 4°C), and the supernatant retained. This process was repeated for the pellet two more times. All three supernatants were then pooled and centrifuged (14,000×*g*, 2 min) in a 0.45 µm ProteomeLab™ spin filter (Beckman Coulter Inc, Fullerton, CA) to remove particulates.

Removal of SDS buffer

Supernatants containing SDS were diluted with one volume of isopropanol. Protein supernatants were separated using kit-based buffers (ProteoSpin™ microcentrifugation detergent clean-up kit, Norgen Biotek Corporation, Ontario, Canada) into basic (pH 8) or acidic (pH 4.5) fractions. Samples were then centrifuged (14,000×*g*, 2 min) on an activated spin column, and proteins were eluted using 50 mM sodium phosphate elution buffer (pH 12.5, 50 µl) into 5 µl of neutralizer solution. Filtrates were maintained at −80°C to prevent protein degradation.

Protein concentration, reduction and cleavage procedures

Total protein content of stone supernatants was determined using a commercial Bradford assay reagent (Bio-Rad Laboratories, Hercules, CA) on a Spectronic 601 spectrophotometer (Milton Roy Company, University Park, PA). Standard curves were constructed using bovine serum albumin. Two to 20 µg of each sample were denatured and reduced, and aliquots of each sample were dried in a speed vacuum. Samples were re-suspended in 20 µl of 0.5 M TEAB (pH 8.5), and proteins denatured with SDS (0.05%) and reduced with TCEP (5 mM) for 1 h at 60°C for basic and acidic proteins. Cysteines were alkylated using 10 mM MMTS at room temperature for 10 min Each sample was then digested with 10 µl of a 1 µg/µl trypsin (Applied Biosystems, Foster City, CA) solution at 37°C overnight. Solutions were then poured into Oasis®MCX extraction cartridges (Waters Corporation, Milford, MA) and gravity filtered through the cartridge to remove trypsin, salts and buffers.

Protein identification by LC-MS/MS

Tryptic peptides (20 mcg of solution) were analyzed by reversed phase, high performance liquid chromatography (RP-HPLC) online with a QSTAR Pulsar *i* quadrapole time of flight (TOF) mass spectrometer as described previously [6]. The peptide elution pattern was assessed upon inspection of total ion chromatogram (TIC) traces. Protein extraction efficiency was presumed efficient and trypsin digest sample was presumed compatible with LC-MS if the TIC elution pattern showed a normal increase in MS signal intensity during gradient elution followed by a drop in signal back to baseline. Tandem mass spectra were searched using Protein Pilot™ 2.0 software, and parameters have been previously described [6]. Protein identifications with confidence limits ≥95% were considered significant. Proteins with <95% confidence or with only one peptide are not reported in this study. All peptide MS/MS spectra from reported proteins were manually inspected.

Results

Stone topographical and mineral composition

X-ray diffraction pattern of matrix stone is shown in the top portion of Fig. 2. The first rounded intensity peak (19°) correlates to the epoxy resin in which the matrix stone was embedded (bottom portion). Peaks marked with an asterisk correlate to biological apatite, identifying the crystalline material contained within the stone as calcium phosphate.

Scanning electron microscopy of matrix stone (Fig. 3) revealed scattered amorphous crystalline material (Fig. 3c). This material is buried within thick, tangential fibrous bands (Fig. 3a, b, e) of protein matrix. At the time of freeze-cracking, portions of these bands were individually identified, measuring 5 μm in width and 40–60 μm in length (Fig. 3e). At higher magnification, bands contained round calcium phosphate deposits (Fig. 3c) and rod-shaped bacteria (Fig. 3d). Laminated, net-like projections can be seen adjacent to two different forms of crystalline material in Fig. 3f.

Protein concentration, RP-HPLC elution, and MS/MS sequencing

Following SDS removal, 1.2 gm of protein was extracted from matrix stone. Two MS–MS samples showed normal elution patterns for peptides separated by RP-HPLC based on individual LC-MS total ion chromatograms (not shown), confirming sample compatibility with C18 chromatography. A total of 33 unique proteins were identified with ≥95% confidence (Table 1). Proteins were then grouped by function by the Gene Ontology Consortium classification system (http://www.geneontology.org).

Of the 33 identified proteins, 24 (73%) are considered inflammatory or involved in inflammatory response. Many, like immunoglobulins, are non-specific humoral responses to foreign bodies. Others, such as elastase, myeloperoxidase, and lysozyme, are more specific to neutrophil response. Plasminogen, hemoglobin, protein C, complement C3, and prothrombin are large plasma proteins that are not typically seen within human urine. They are likely present from bleeding and localized stone trauma.

Discussion

Matrix stones have been described more commonly in female populations [7, 8] and in patients with stone

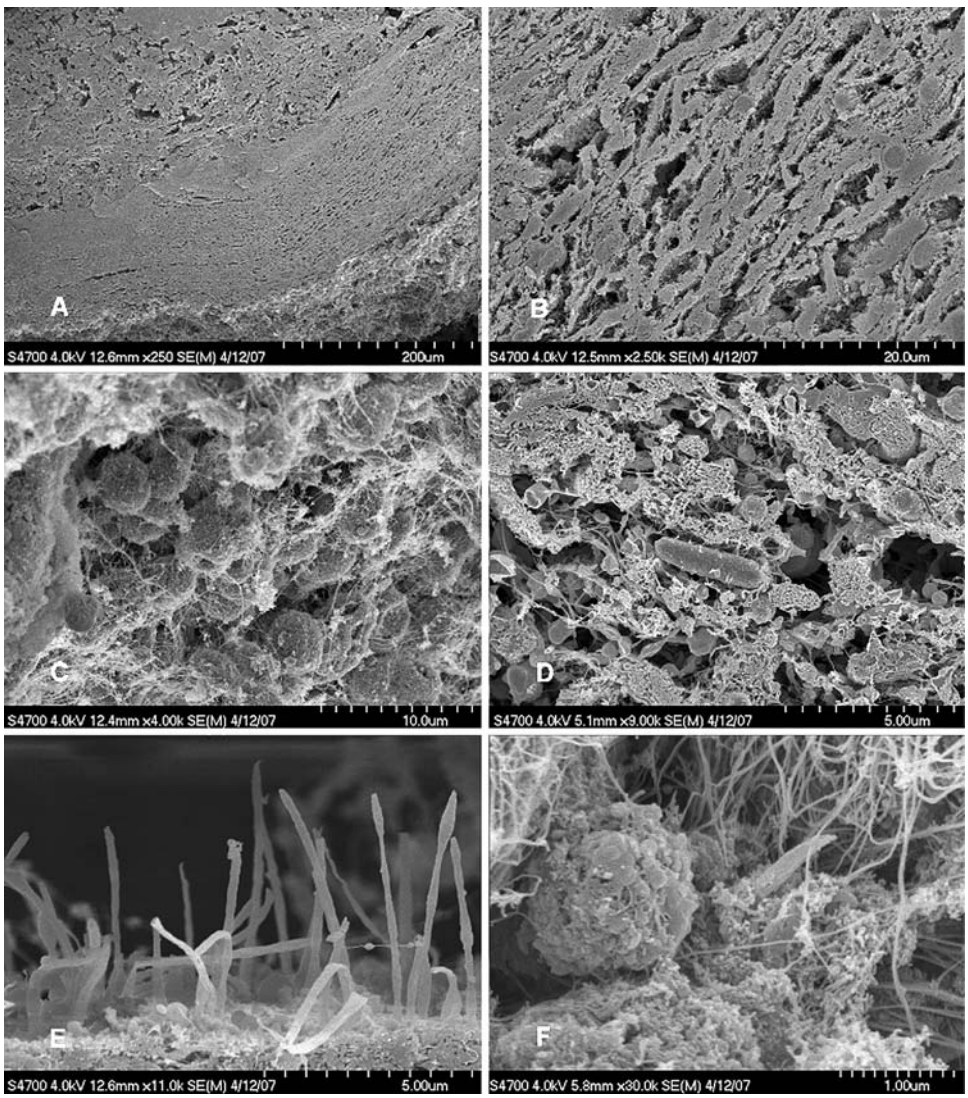

Fig. 3 Scanning electron microscopy of matrix stone. Crystalline material (**b**, **c**, **f**) and rod-shaped bacteria (**d**) are seen buried within tangential fibrous bands (**a**, **e**)

Table 1 Identified proteins in one human matrix stone

Category/protein	% coverage	GI accession	pI	kDa
Cell biogenesis/membrane/structure				
Histone 1	8	9863664	11.4	11.4
Tamm-Horsfall protein	12	137116	5.1	69.8
Coagulation				
Protein C	4	763120	5.9	52.1
Prothrombin	6	67624831	5.7	70.0
Defense/immune response				
α1 anti-trypsin	6	28966	5.4	46.7
Anti-TNF α antibody	8	13774112	8.9	23.4
Azurocidin 1	14	62739619	9.8	26.9
Calgranulin A	45	30583595	6.5	10.8
Calgranulin B	57	56205191	5.7	13.1
Cathepsin G	10	179915	11.2	28.8
Complement C3	6	40786791	6.0	187
Defensin alpha-1	10	85567619	6.5	10.2
Eosinophilic cationic protein	9	11139050	10.3	18.4
Ig light chain	38	90109489	8.6	23.2
IgG2	35	2414498	4.6	7.2
IgG heavy chain	20	59809002	8.6	51.6
IgG protein	26	229601	8.8	48.2
Ig kappa chain	36	33604108	8.6	25.7
Ig kappa light chain	14	8918520	7.8	23.3
Lactoferrin	41	186833	8.5	78.2
Lysozyme C	11	48428997	8.4	16.4
Myeloblastin	5	188984	8.5	23.6
Myeloperoxidase	16	88180	9.3	92.4
Neutrophil elastase	14	119292	9.7	28.5
Neutrophil lipocalin	33	4261868	9.0	20.5
Orosomucoid (α1A glycoprotein)	12	998943	4.9	23.5
Radixin	4	4506467	6.0	68.6
Thioredoxin peroxidase α chain	22	9955007	5.7	21.8
Plasma				
Albumin	5	23243418	6.1	66.9
Histidine-rich glycoprotein	2	47479594	7.1	59.6
Plasminogen	8	56203917	7.0	90.5
Transport				
Hemoglobin alpha chain	46	999565	8.7	15.1
Hemoglobin beta chain	24	999567	8.0	15.9

GI GenBank Identifier number is associated with NCBI protein database, http://www.ncbi.nlm.nih.gov/entrez, *pI* isoelectric point, *kDa* kilodalton weight

histories [9]. Dialysis patients with persistent proteinuria are also thought to be at risk of matrix stone development [3, 9], although one series reported associated urinary tract infections in all three of their dialysis patients with matrix stones [9]. In 1956, Boyce and Garvey analyzed pooled crystalline and matrix calculi and subjected them to amide hydrolysis, converting organic peptides into amino acids [10]. In their analysis, threonine and leucine were the principal amino acid components across all stone types, with serine, tyrosine, arginine, and lysine found in smaller quantities. They concluded that the matrix substances from crystalline stones were almost identical to the organic substances found within matrix stones, but they were uncertain why matrix calculi did not calcify [10]. Despite over 40 years of research in this area, the question of whether protein contained within kidney stones is essential in calculogenesis [11] or just an innocent bystander in a largely mineral process [12] has not been answered. Proponents of the latter would have difficulty explaining matrix stones on a purely mineralogic basis, as matrix stones are composed

primarily of mucoproteins and carbohydrates, with crystal deposited as the inclusion material. In addition, the risk factors associated with matrix stone formation (infection with urease splitting organisms, urinary stasis, and proteinuria) also seem to predispose patients to calcium or struvite kidney stones [13].

The SEM findings of orderly, structured laminated bands suggest that the stone grew intermittently and slowly in a solution highly saturated with protein. Calcium phosphate deposits scattered throughout the entire structure imply that the fibrous bands formed first, devoid of a significant mineral phase. The microfibrillar pattern seen in the freeze-cracked Fig. 3e has been previously demonstrated in non-infected matrix stones of dialysis patients [3] but not in a matrix stones associated with Proteus infection. The thin, microfibrillar elements do not resemble the classic striation pattern of fibrin, and indeed, our proteomic analysis did not reveal fibrin or fibrinogen. This finding is supported by multiple other matrix stone studies with negative immunofluorescence staining and amino acid analysis for fibrin [3, 13]. If not fibrin, it is possible these bands may represent precipitated Tamm–Horsfall glycoprotein (THP). This excretory urinary protein has been demonstrated to be a constitutive inhibitor of calcium crystallization within urine in renal fluids as well as a defense modulator against uropathogenic bacteria [14]. It is known for its notorious ability to self-aggregate and to activate human neutrophils through a single class of sialic acid-specific cell surface receptors [15]. Perhaps in this patient, THP precipitated and was partly responsible for initiating the inflammatory activation of human polymorphonuclear leukocytes within the urine.

Neutrophil granulocyte, monocytes, and tissue macrophages are cytotoxic cells critical in defense against bacteria. When stimulated, they can secrete primary (azuorphlic) granules containing proteolytic enzymes such as cathepsin G, elastase [16], myeloperoxidase [17], and lysozyme [17] or secondary granules with a variety of components such as lactoferrin [18], lysozyme, calprotectin, collagenase, and lipocalins [19]. All of these proteins were identified within matrix stone (Table 1), an inflammatory fingerprint of neutrophil involvement within the collecting system.

Mechanistically, renal tubular epithelial cells can also react to stimulated macrophages and cytokines by upregulating osteopontin, calprotectin, or other calcium-binding molecules as a protective mechanism against crystalluria and stone formation [20]. The common urinary protein osteopontin was not identified within matrix stone, suggesting that the stone's origin was the collecting system rather than the nephron.

To our knowledge, this is the first attempt to identify all the proteins found within a matrix stone, and, since most matrix stones are formed in the setting of active urinary tract infections, the predominance of inflammatory proteins is not surprising. Recently, using an MS-based approach, three different groups out of three different labs have reported more than 100 identifiable proteins within kidney stone matrix extracted from powdered calcium oxalate stones [6, 21, 22]. Interestingly, all three groups report a predominance of defense and inflammatory proteins, and more than half of the proteins described in calcium oxalate stone matrix were also observed within this matrix stone. This finding suggests that matrix might serve as a template or precipitant for secondary crystal deposition. Of course, the presence of these proteins does not prove causality, as the matrix may have become attached to cell membrane proteins during passage/surgery or been contaminated with serum proteins from bleeding within the urinary tract. However, it does appear that similar inflammatory pathways are involved in the generation and/or accumulation of matrix products within both matrix and crystalline calculi.

The largest limitation of this study is the analysis of a single matrix stone. As this stone was associated with Proteus UTI, it would have been helpful to compare a proteome of Proteus-associated struvite stone, but we have yet to establish this proteome. In addition, our group evaluated the presence or absence of a particular protein, not the quantity of protein identified. It is possible that we underreported proteins, missed important information regarding protein concentration, or failed to detect proteins of low molecular weight. We are confident that we limited false positive proteins by stringent tandem MS methods.

In conclusion, matrix stones are organized by structured, laminated bands devoid of significant crystal deposits. Their protein profile includes many of the same inflammatory proteins seen in previous MS studies of calcium oxalate stone matrix. In addition to reporting more than 30 new proteins within matrix stones, our findings indicate a primary inflammatory mechanism behind matrix stones. More study is needed on matrix stones from other non-infected populations to further clarify causality.

Acknowledgments B.K.C. is supported by a Foundation Research Scholar Grant from the American Urological Association and a Biomedical Genomics Center Seed Grant from the University of Minnesota. I.W.K. is supported by the Soongsil University Research Fund.

References

1. Boyce WH, Sulkin NM (1956) Biocolloids of urine in health and in calculous disease. III. The mucoprotein matrix of urinary calculi. J Clin Invest 35:1067–1079
2. Gage H, Beal HW (1908) V. Fibrinous Calculi in the Kidney. Ann Surg 48:378–387
3. Bommer J, Ritz E, Tschope W, Waldherr R, Gebhardt M (1979) Urinary matrix calculi consisting of microfibrillar protein in patients on maintenance hemodialysis. Kidney Int 16:722–728

4. Wilson RM, Elliott JC, Dowker SEP (1999) Rietveld refinement of the crystallographic structure of human dental enamel apatites. Am Minerol 84:1406–1414
5. Zhang W, Ratcliffe CI, Moudrakovski IL, Mou CY, Ripmeester JA (2005) Distribution of gallium nanocrystals in Ga/MCM-41 mesocomposites by continuous-flow hyperpolarized 129Xe NMR spectroscopy. Anal Chem 77:3379–3382
6. Canales BK, Anderson L, Higgins L, Slaton J, Roberts KP, Liu N, Monga M (2008) Second prize: comprehensive proteomic analysis of human calcium oxalate monohydrate kidney stone matrix. J Endourol 22:1161–1167
7. Stoller ML, Gupta M, Bolton D, Irby PB 3rd (1994) Clinical correlates of the gross, radiographic, and histologic features of urinary matrix calculi. J Endourol 8:335–340
8. Rowley MW, Faerber GJ, Wolf JS Jr (2008) The University of Michigan experience with percutaneous nephrostolithotomy for urinary matrix calculi. Urology 72:61–64
9. Shah HN, Kharodawala S, Sodha HS, Khandkar AA, Hegde SS, Bansal MB (2009) The management of renal matrix calculi: a single-centre experience over 5 years. BJU Int 103:810–814
10. Boyce WH, Garvey FK (1956) The amount and nature of the organic matrix in urinary calculi: a review. J Urol 76:213–227
11. Boyce WH, King JS Jr (1959) Crystal-matrix interrelations in calculi. J Urol 81:351–365
12. Finlayson B, Vermeulen CW, Stewart EJ (1961) Stone matrix and mucoprotein from urine. J Urol 86:355–363
13. Koide T, Miyagawa M, Kinoshita K (1977) Matrix stones. J Urol 117:786–787
14. Hession C, Decker JM, Sherblom AP, Kumar S, Yue CC, Mattaliano RJ, Tizard R, Kawashima E, Schmeissner U, Heletky S et al (1987) Uromodulin (Tamm-Horsfall glycoprotein): a renal ligand for lymphokines. Science 237:1479–1484
15. Thomas DB, Davies M, Peters JR, Williams JD (1993) Tamm Horsfall protein binds to a single class of carbohydrate specific receptors on human neutrophils. Kidney Int 44:423–429
16. Ohlsson K, Olsson I (1974) The neutral proteases of human granulocytes. Isolation and partial characterization of granulocyte elastases. Eur J Biochem 42:519–527
17. Hansen NE, Karle H, Andersen V, Malmquist J, Hoff GE (1976) Neutrophilic granulocytes in acute bacterial infection. Sequential studies on lysozyme, myeloperoxidase and lactoferrin. Clin Exp Immunol 26:463–468
18. Reiter B (1983) The biological significance of lactoferrin. Int J Tissue React 5:87–96
19. Carlson M, Raab Y, Seveus L, Xu S, Hallgren R, Venge P (2002) Human neutrophil lipocalin is a unique marker of neutrophil inflammation in ulcerative colitis and proctitis. Gut 50:501–506
20. Kohri K, Nomura S, Kitamura Y, Nagata T, Yoshioka K, Iguchi M, Yamate T, Umekawa T, Suzuki Y, Sinohara H et al (1993) Structure and expression of the mRNA encoding urinary stone protein (osteopontin). J Biol Chem 268:15180–15184
21. Chen WC, Lai CC, Tsai Y, Lin WY, Tsai FJ (2008) Mass spectroscopic characteristics of low molecular weight proteins extracted from calcium oxalate stones: preliminary study. J Clin Lab Anal 22:77–85
22. Merchant ML, Cummins TD, Wilkey DW, Salyer SA, Powell DW, Klein JB, Lederer ED (2008) Proteomic analysis of renal calculi indicates an important role for inflammatory processes in calcium stone formation. Am J Physiol Renal Physiol 295:F1254–F1258